Journal of *Marine Science and Engineering*

MDPI

Article

Fatigue Analysis for Shaft of Inland River Ship Under Ice Load

Kai Yang [1,2,*] and Guoqing Feng [1]

[1] College of Shipbuilding Engineering, Harbin Engineering University, Harbin 150001, China; fengguoqing@hrbeu.edu.cn
[2] China Classification Society-Harbin Branch, Harbin 150070, China
* Correspondence: yangkai05011713@163.com

Abstract: Inland river ships navigating in an ice area cannot avoid contact between the propeller and ice block. In addition to ensuring the safety of propeller blades, the fatigue strength of the propulsion shaft system under ice load excitation must also be considered. This paper first studies how to calculate the natural frequency of free torsional vibration of the system, then uses Newmark integral programing to calculate the maximum torsional stress of shaft system under ice load at resonance speed. Low cycle stress and high cycle stress are studied according to fatigue analysis theory. The method of determining S–N curve and ice load stress spectrum is given and the cumulative damage ratio is calculated based on Palmgren–Miner linear cumulative damage theory. Finally, taking a real inland river vessel propulsion shaft system as an example, the fatigue strength of the shaft system under different working conditions of ice load excitation is studied. Therefore, this study has practical significance and engineering application value in conducting fatigue research on the propulsion shaft system of an inland waterway vessel sailing in an ice area.

Keywords: ice load; propulsion shaft; fatigue strength; torsional stress; cumulative damage ratio

Academic Editor: Md Jahir Rizvi

Received: 26 December 2024
Revised: 8 January 2025
Accepted: 11 January 2025
Published: 13 January 2025

Citation: Yang, K.; Feng, G. Fatigue Analysis for Shaft of Inland River Ship Under Ice Load. *J. Mar. Sci. Eng.* **2025**, *13*, 131. https://doi.org/10.3390/jmse13010131

1. Introduction

The northeast region of China experiences an annual river ice period, so studying the fatigue characteristics of the propulsion shaft system of ships sailing during the ice period is of great significance for the safety of ships. The "RCIWSS" [1] specifies that, when the single unit power of the ship's main engine exceeds 220 kW, it is necessary to verify the torsional vibration of the propulsion shaft system. Ships sailing in ice areas will be hit by ice blocks; they cause a huge torsional excitation of the shaft system [2]. Prolonged exposure to the impact torque will cause fatigue damage to the shaft system, which is different from the fatigue strength analysis of the shaft system under steady-state operation. At present, the fatigue calculation of the propulsion shaft system for inland river ships sailing in ice areas is blank, and there are currently no calculation methods or complete fatigue analysis calculation processes for the S–N curve of propulsion shaft system for inland river ships sailing in ice areas. The innovation and objective of this article lie in investigating the fatigue behavior of instantaneous torsional stress within the shaft system of inland waterway vessels subsequent to ice impact on their propellers. Distinct from previous research, which predominantly examined the stable torsional stress in shaft systems powered exclusively by diesel engines, this research delves into a novel area.

Yang [3] studied the multi-axial fatigue assessment method of polar ships under ice loading. Based on the key techniques of ship–ice–water coupling numerical simulation, the mechanism of ship–ice collision under typical conditions is analyzed, and the effects of

ice density and ship speed on ice motion, ice load curve and energy curve are discussed. Based on the numerical simulation results, the fatigue assessment position is selected and the multi-axial fatigue analysis sub-model is established. The dynamic response of the structure is analyzed by applying ice load, and the multi-axial fatigue damage of polar ships is evaluated by combining the ice-induced multi-axial fatigue assessment method. Chen [4] established the equivalent shaft model; then, free vibration and forced vibration analyses are calculated. "Dangerous rotational speed" of the propulsion shafting can get from the result. Based on Matlab, the transient response of the propulsion shafting under dangerous rotational speed is analyzed and the dynamic characteristics of the propulsion shafting also can be obtained from the transient result. Based on Ansys Workbench, the transient dynamics of the helical gear pair are analyzed and the fatigue life of the helical gear pair is calculated. Wu et al. [5] calculated the spatial co-ordinates of the characteristic points on the tangent plane of the blade and completed the model establishment of the blade in Pro/Engineer. Sun et al. [6] eliminated the complex transformation of plane and spatial co-ordinates and used Pro/E to create curves and merge surfaces, achieving the most intuitive modeling. In addition, they can verify initial data and update incorrect parameters in the establishment of blade models, efficiently establishing blade models. Qian et al. [7] utilized MSC. Patran's secondary developed technology to automatically establish the three-dimensional model and finite element of blade, avoiding repetitive and complex preprocessing work and improving analysis efficiency. Hu [8] elaborated on the empirical formula of classification society for propeller verification, established a three-dimensional model of the propeller, and constructed an ice/propeller contact model to perform finite element calculations on the strength of the propeller under ice load. They also conducted relevant analysis on the dynamic response of the propeller during the impact process. Wu used ABAQUS(2016) finite element software to conduct time–domain response analysis of the shaft system and verified the feasibility of the numerical calculation method for shaft vibration. Wu [9] conducted a sensitivity analysis of the torsional vibration for the main components of the shaft system, such as the stiffness of coupling and the inertia of clutch, to verify the feasibility of the numerical calculation method for shaft vibration. Xiao et al. [10] constructed a mathematical model of complex shaft torsional vibration based on the basic models of straight chain and branched torsional vibration. Murawski et al. [11] introduce the measurement of crankshaft torsional vibration in marine engines under simulated faults. The given test results are from a test cycle conducted on a laboratory bench at the Maritime University of Gdynia, which is equipped with a three-cylinder self-ignition engine to power the generator. The device being developed by Sibryaev et al. [12] will allow for continuous monitoring for the level of torsional vibration. If torsional vibration increases, a signal will be sent to the ship mechanic to switch to another operating mode of the main engine, which will improve the reliability and automation of the ship's power plant and enhance navigation safety. Kettrakul et al. [13] analyzed the severely fractured transmission shaft after 2 years of use and found that there was reverse bending fatigue, and the fracture of the transmission shaft was clearly a low-stress fatigue fracture. Han et al. [14] verified that high torsional vibration of the propulsion shaft system caused by lateral torsional coupling vibration can lead to fatigue fracture of the shaft. It is necessary to limit this torque through analytical calculations and experimental verification, and estimate the fatigue stability and life cycle of the shaft using the Soderberg method and linear damage accumulation method. Li [15] analyzed the phase effect between diesel engine excitation and ice load excitation and solved the torsional vibration response of the propulsion shaft system under ice load excitation using the Newmark method. DNV-GL Group has developed a software module, Nauticus Machinery(14.4), for fatigue calculation of the propulsion shaft system under ice load. Gao et al. [16] studied collision avoidance

decision-making research in coastal waters considering the uncertainty of target ships. Lee et al. [17] presented a fundamental technique for analyzing ice loads in the frequency domain based on data measured at various angles in the ice-water tank experiment. Shen et al. [18] conducted uniaxial unconfined compressive strength tests on river ice in different regions of Heilongjiang Province and, combined with existing research results on river ice compressive strength in China, analyzed the influence of ice temperature and strain rate on compressive strength and provided suggestions for the standard values of river ice compressive strength in various regions of Heilongjiang Province. Based on the FEM calculation of the static strength under two groups of alternating ice loads, Wang et al. [19] analyzed the fatigue performance of a PC2 ice-class propeller under the fatigue criterion of stress–frequency spectrum and the criterion of cumulative fatigue damage, respectively. A feasible calculation method for the fatigue strength of the ice-class propeller is proposed to analyze the effects of propeller skew, rake, hydrofoil profile, and mean stress correction on fatigue performance. Xu et al. [20] introduced the experimental research on ice-propeller milling under different ice materials, propeller size, milling depth, ice moving velocity and propeller rotation speed, which was carried out by use of the ice-propeller milling test platform. The propeller ice load, shadowing effect and ice-propeller action mode were measured and analyzed. Chen et al. [21] simulated the ice cone and rigid body collision test to verify the feasibility of the calculation method. Wu et al. [22] simulated a three-dimensional propeller based on the multiple reference frame and Messinger thermodynamic model to analyze the effect of the anti-icing heat load. At present, a large amount of research studies the fatigue strength of ship structures under ice load, but there is no relevant literature on the fatigue strength of ship shaft systems under ice load.

This article first introduces how to calculate the instantaneous torsional stress of the propulsion shaft system under ice load and then describes the calculation methods of low cycle stress and high cycle stress, as well as how to determine the S–N curve of the shaft system itself, the ice load stress spectrum, and the fatigue cumulative damage ratio. Finally, taking the propulsion shaft system of an inland waterway ship as an example, the research method and corresponding conclusions are explained in detail.

2. Calculation of Instantaneous Torsional Stress of Shaft System Under Ice Load

To calculate free torsional vibration, it is first necessary to establish the motion equation of the torsional vibration system, and the actual ship power plant system is shown in Figure 1. The crank, flange, gearbox, shaft, propeller and other important components in the propulsion system are simplified into related mass points. For ease of calculation, each mass point can be modeled as a moment of inertia $\boldsymbol{J}$, and the direct connection between two mass points can be modeled as a damping matrix $\boldsymbol{C}$ and a stiffness matrix $\boldsymbol{K}$.

The methods for studying free vibration of shaft systems include modal analysis, Rayleigh's method, and the field matrix method. Modal analysis is a method of revealing the vibration characteristics of a shaft system by calculating its natural frequencies and mode shapes. It is based on linear vibration theory and obtains the natural frequency and corresponding vibration mode by solving the characteristic equation of the system. Rayleigh's method is an analysis method based on the principle of energy conservation, which can be used to solve the natural frequency and dominant mode of a system. The field matrix method is commonly regarded as a chain-like structure composed of multiple units in a system. The interactions between these units can be described by transfer matrices, and the vibration characteristics of the entire system can be further analyzed by solving the system matrices obtained from these transfer matrices.

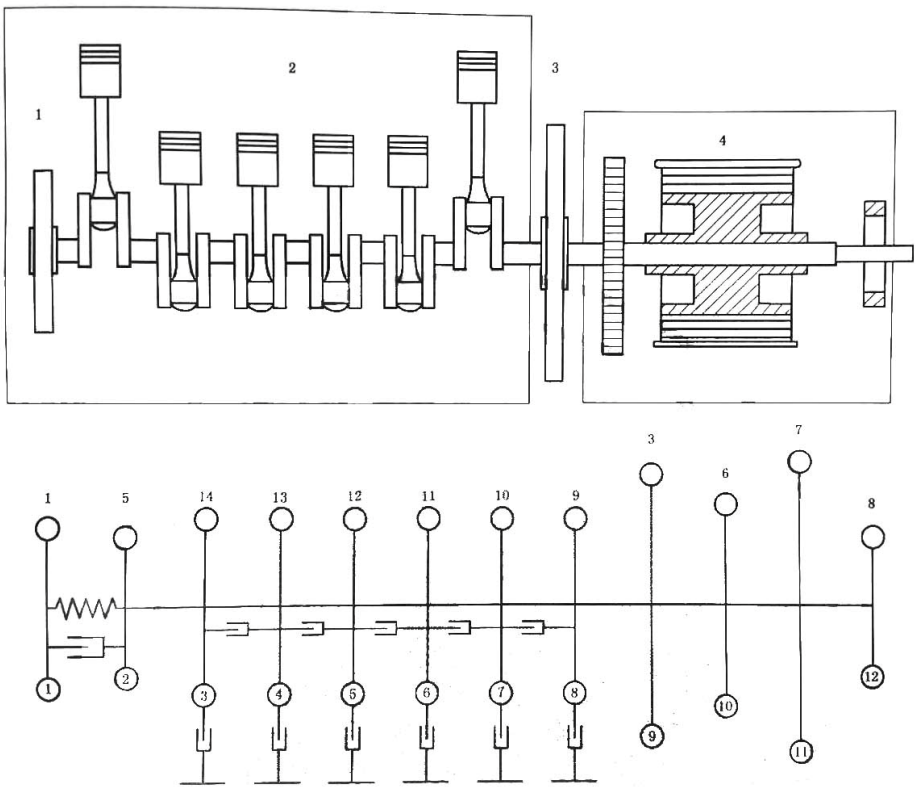

Figure 1. Actual ship power plant system.

It uses the field matrix method to solve free vibration of the system, and $\lambda = \omega_n{}^2$, $\boldsymbol{H} = \boldsymbol{J}^{-1}\boldsymbol{K}$, where $\boldsymbol{J}$ is the inertia matrix and $\boldsymbol{K}$ is the stiffness matrix; ω_n is the nth order natural frequency of the system. Solving the matrix equation $(\boldsymbol{H} - \lambda \boldsymbol{E})\boldsymbol{A} = 0$, the eigenvalues obtained from this equation can be used to obtain natural frequencies for each order, and the eigenvector corresponding to each eigenvalue is the relative amplitude of different mass numbers at that natural frequency.

When the ice hits the propeller, it causes significant torsional stress on the shaft system. However, the torsional excitation of ice load is a nonperiodic load, and traditional frequency domain methods cannot be used to solve the dynamic response. It is necessary to study from the time–domain method to calculate the transient response of the shaft system under ice load impact. To shorten the calculation time and improve the calculation accuracy and efficiency, an efficient stepwise integration method can be used for numerical simulation calculations [23]. The present work adopts the Newmark integration method, and the integration format is as follows:

$$\{\ddot{x}\}_{n+1} = \frac{1}{\beta\Delta t^2}(\{x\}_{n+1} - \{x\}_n) - \frac{1}{\beta\Delta t}\{\dot{x}\}_n - (\frac{1}{2\beta} - 1)\{\ddot{x}\}_n \tag{1}$$

$$\{\dot{x}\}_{n+1} = \frac{\gamma}{\beta\Delta t}(\{x\}_{n+1} - \{x\}_n) + (1 - \frac{\gamma}{\beta})\{\dot{x}\}_n - (1 - \frac{\gamma}{2\beta})\{\ddot{x}\}_n \tag{2}$$

$$[\overline{K}] = [K] + \frac{1}{\beta\Delta t^2}[J] + \frac{\gamma}{\beta\Delta t}[C] \tag{3}$$

$$\left\{\overline{f}\right\}_{n+1} = \{f\}_{n+1} + [J][\frac{1}{\beta\Delta t^2}\{x\}_n + \frac{1}{\beta\Delta t}\{\dot{x}\}_n + (\frac{1}{2\beta} - 1)\{\ddot{x}\}_n] + [C][\frac{\gamma}{\beta\Delta t}\{x\}_n + (\frac{\gamma}{\beta} - 1)\{\dot{x}\}_n + (\frac{\gamma}{2\beta} - 1)\Delta t\{\ddot{x}\}_n] \tag{4}$$

$$[\overline{K}]\{x\}_{n+1} = \left\{\overline{f}\right\}_{n+1} \tag{5}$$

where $\beta = \gamma = 0.5$ and Δt is not greater than one tenth of the minimum vibration period.

$[K]$ is the stiffness matrix of the system, $[J]$ is the matrix of the system's moment of inertia, $[C]$ is the damping matrix of the system, and $\{f\}_{n+1}$ is the current external torque. By using software programing to solve linear Equation (5), the current displacement value $\{x\}_{n+1}$ can be obtained. By inputting the results into Equations (1) and (2), the current velocity $\{\dot{x}\}_{n+1}$ and acceleration $\{\ddot{x}\}_{n+1}$ can be calculated, thus completing a one-step calculation [24].

The damping of a low-speed diesel engine propulsion shaft system mainly includes diesel engine damping and propeller damping. Typical propeller damping models include the Archer model and Prodam model; the analysis adopts the Archer damping model [25].

The formula for the damping coefficient of a propeller is as follows [26]:

$$C_p = \frac{9542 a N_p N_c}{n_e^2} \quad \text{N·m·s/rad} \tag{6}$$

where N_p is power absorbed by the propeller at rated speed, n_e is rated speed, N_c is propeller speed at critical operating conditions, and a is the coefficient; the specific formula is as follows:

$$a = 5\frac{A}{A_d}\cdot\frac{H}{D}\left[\frac{\frac{H}{D}+0.5}{0.0066\left(A_g+2\frac{A}{A_d}\right)\left(\frac{A}{A_d}+\frac{1}{2Z_p}\right)}+V\right] \tag{7}$$

where $\frac{A}{A_d}$ is the expanded blade area ratio, $\frac{H}{D}$ is the pitch ratio, Z_p is the number of blades, when $Z_p = 4$, $V = 1$, and A_g is moment coefficient; the specific formula is as follows:

$$A_g = 33.985 \times 10^6 \frac{N_p}{n_e^3 D^5} \tag{8}$$

where D is propeller diameter.

The loads that cause instantaneous torsional vibration of the shaft system are mainly the diesel engine load and the ice-induced propeller load. The diesel engine load is calculated at the corresponding cylinder mass point based on the ignition interval angle of different cylinders and is compared with the torsional time. The ice-induced propeller load is directly loaded onto the propeller particle, forming an external force matrix for different time periods $\{f\}_n$. The load formula for diesel engines is as follows [22]:

$$M = \sum M_\nu \sin(\nu\omega t + \varphi_\nu) \quad \text{N·m} \tag{9}$$

where $M_\nu = \frac{\pi D^2 R C_\nu}{4}$, φ_ν-v is order initial phase angle, and $\varphi_\nu = \arctan\left(\frac{a_\nu}{b_\nu}\right)$.

Using each time period, it calculates the torque values for each order and then sums them up to obtain the torque value for that time period. Comparing the firing angle position for that time period, it assigns the torque value to the corresponding cylinder mass point and improves the external force matrix $\{f\}_n$.

The formula for designing maximum torque of ice blocks is as follows [27]:

$$\text{For } D \le D_{limit},\ Q_{max} = 10.9\left(1-\frac{d}{D}\right)\left(\frac{P_{0.7}}{D}\right)^{0.16}(nD)^{0.17}D^3 \quad \text{kN·m}$$

$$\text{For } D > D_{limit},\ Q_{max} = 20.7\left(1-\frac{d}{D}\right)\left(\frac{P_{0.7}}{D}\right)^{0.16}(nD)^{0.17}D^{1.9}H_{ice}^{1.1} \quad \text{kN·m} \tag{10}$$

where $D_{limit} = 1.8H_{ice}$, H_{ice} is maximum design ice thickness, d is outer diameter of the propeller hub, $P_{0.7}$ is pitch at 0.7R of the propeller, and n is rotational propeller speed at MCR in bollard condition; it is $0.85n_e$ when it is driven by diesel engine.

The instantaneous torque formula for the impact of ice load on the propeller is as follows:

$$\varphi = 0 \ldots \alpha_i,\ Q(\varphi) = C_q Q_{\max}[\varphi(180/\alpha_i)] \quad \text{kN·m}$$
$$\varphi = \alpha_i \ldots 360,\ Q(\varphi) = 0 \quad \text{kN·m} \tag{11}$$

where C_q is the ice impact magnification factor, φ is the start of the rotation angle of the first ice impact, and α_i is the duration of interaction between propeller blades and ice measured by rotation angle.

The values of C_q and α_i are shown in Table 1.

Table 1. Values of C_q and α_i.

Torque Excitation	Propeller/Ice Interaction	C_q	α (°)			
			$Z = 3$	$Z = 4$	$Z = 5$	$Z = 6$
Case 1	Single ice block	0.75	90	90	90	72
Case 2	Single ice block	1.0	135	135	135	135
Case 3	Two ice blocks (phase shift 360°/2/Z)	0.5	45	45	36	30
Case 4	Single ice block	0.2	45	45	36	30

A plot of all excitation cases for different numbers of blades is given in Figures 2 and 3.

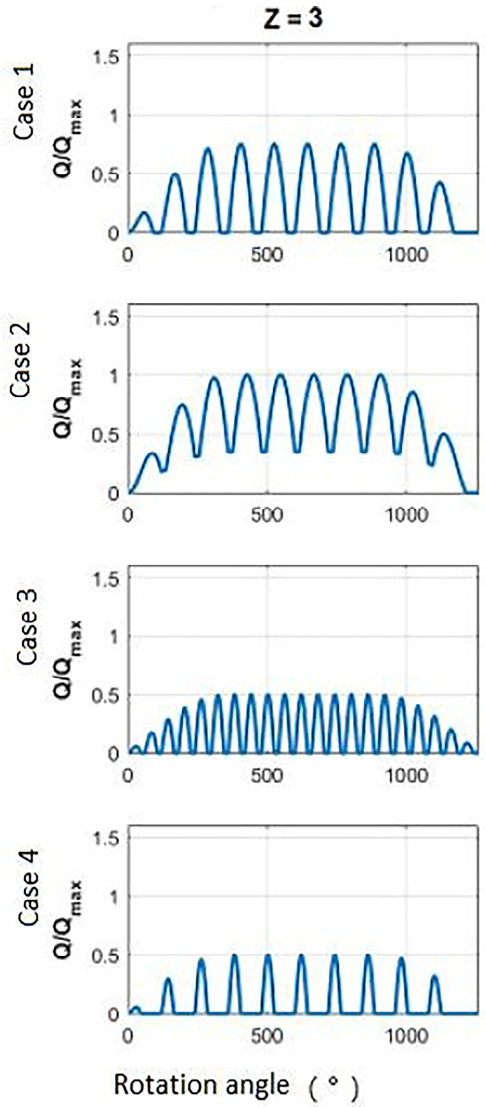

Figure 2. The shape of the propeller ice torque excitation sequences for propellers with 3 blades.

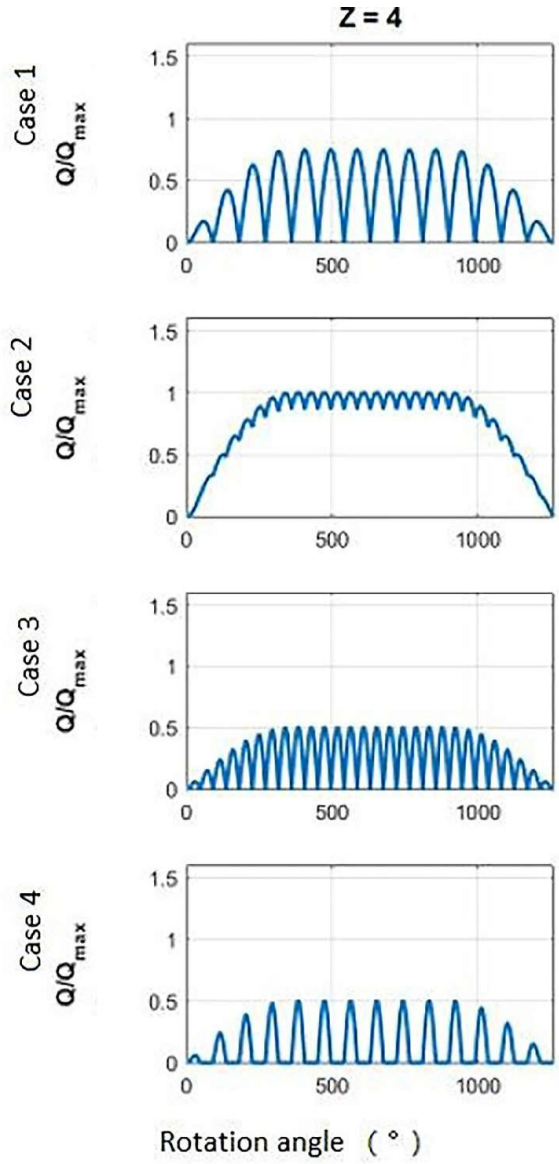

Figure 3. The shape of the propeller ice torque excitation sequences for propellers with 4 blades.

3. Low Cycle Stress Calculation

When there is no ice load and cycles are fewer than 10^4, the maximum stress τ_{max} of the shaft system needs to meet [28]:

$$\tau_{max} \leq \frac{\sigma_y}{2S_L K_L} \tag{12}$$

where σ_y is material yield strength, S_L is low cycle safety factor, which is 1.25, K_L is the low cycle impact coefficient; it is calculated according to Formula (13).

$$K_L = 1 + (\alpha_t - 1)\frac{\sigma_y}{900} + 10^{-4}(\sigma_B - 200)\lg R_y \tag{13}$$

where α_t is the stress concentration factor, which is calculated according to Formula (14), σ_B is tensile strength, and R_y is surface roughness of shaft.

$$\alpha_t = 1 + \frac{1}{\sqrt{6.8\frac{r}{D-d} + 38\frac{r}{d}(1+2\frac{r}{d})^2 + 4\frac{d}{D}(\frac{r}{D-d})^2}} \tag{14}$$

where r is transition arc radius, D is flange diameter, and d is shaft diameter.

The maximum stress τ_{max} of the shaft system is calculated by Formula (15):

$$\tau_{max} = \tau_0 K_A \quad \text{MPa} \tag{15}$$

where τ_0 is nominal torsional stress at rated power, which is calculated according to Formula (16), and K_A is the repetitive cycle torque coefficient, which is 1.3.

$$\tau_0 = \frac{T_0}{W} \qquad \text{MPa} \tag{16}$$

where T_0 is torque at rated power, which is calculated according to Formula (17), and W is shaft section modulus.

$$T_0 = \frac{9545.45 N_e}{n} \times 1000 \quad \text{kN·m} \tag{17}$$

where N_e is the rated power of the diesel engine and n is the rated speed of the diesel engine.

4. High Cycle Stress Calculation

When there is no ice load and cycles are more than 3×10^6, the torsional stress τ_v of the shaft system needs to meet:

$$\left(\frac{\tau_v}{\tau_f}\right)^2 \leq \frac{1}{S_Q{}^2} \tag{18}$$

where τ_f is high cycle torsional fatigue strength, which is calculated according to Formula (19), and S_Q is high cycle safety factor, which is 1.25.

$$\tau_f = \frac{0.24\sigma_y + 42 - 0.15\tau}{K_{H\tau}} \qquad \text{MPa} \tag{19}$$

where τ is nominal torsional stress, which is τ_0 at rated speed, $K_{H\tau}$ is the high cycle impact coefficient, which is calculated according to Formula (20).

$$K_{H\tau} = \frac{\alpha_t}{m_t} + 0.01\sqrt{r} + 3 \times 10^{-4}(\sigma_B - 100)\lg R_y \tag{20}$$

where m_t is the high cycle torsional fatigue sensitivity coefficient; it is calculated according to Formula (21).

$$m_t = 1 + \left(\frac{60}{\sigma_y} + 0.05\right)\sqrt{\frac{1}{r}} \tag{21}$$

where r is the minimum value of the cut radius or shaft radius; when r is greater than 100 mm, it is taken as 100 mm.

Shaft torsional stress τ_v can be calculated by Formula (22):

$$\tau_v = (K_{Anorm} - 1)\tau_0 \quad \text{MPa} \tag{22}$$

where K_{Anorm} is the repetitive cycle torque coefficient under normal operation, which is 1.2.

5. Determining S–N Curve

For the fatigue strength analysis of shaft systems in navigation ice areas, based on Palmgren–Miner linear cumulative damage theory, a double-slope S–N curve is adopted. Firstly, it is necessary to determine the stress amplitudes of high cycle and low cycle. Low cycle stress amplitude τ_{vLC} for 10^4 cycles is calculated according to Formula (23):

$$\tau_{vLC} = \frac{\sigma_y}{2S_{vLC}K_L} - \tau \qquad \text{MPa} \tag{23}$$

where τ is nominal torsional stress, which is $\left(\frac{n}{n_0}\right)^2 \tau_0$, and n is resonant speed.

High cycle stress amplitude τ_{vHC} for 3×10^6 cycles is calculated according to Formula (24):

$$\tau_{vHC} = \frac{\tau_f}{S_Q} \quad \text{MPa} \tag{24}$$

where S_Q is high cycle safety factor, which is 1.25; for $N = 10^9$, it is 1.5.

When the number of cycles $N \leq 3 \times 10^6$, the relationship between the number of cycles and stress amplitude is shown in Formula (25) [29]:

$$N_1(\tau_{vice}) = \overline{\alpha_1}\tau_{vice}^{-m_1} \tag{25}$$

where $\overline{\alpha_1} = 3 \times 10^6 \tau_{vHC}^{m_1}$, $m_1 = \frac{\lg(10^4/(3\times10^6))}{\lg(\tau_{vHC}/\tau_{vLC})}$.

When the number of cycles $N > 3 \times 10^6$, the relationship between the number of cycles and stress amplitude is shown in Formula (26):

$$N_2(\tau_{vice}) = \overline{\alpha_2}\tau_{vice}^{-m_2} \tag{26}$$

where $\overline{\alpha_2} = 3 \times 10^6 \tau_{vHC}^{m_2}$, $m_2 = \frac{\lg(3\times10^6/10^9)}{\lg(\tau_f/1.5\tau_{vHC})}$.

Based on the co-ordinate points associated with τ_{vLC} and τ_{vHC} and using the calculated value of τ_{vice} at 10^9 cycles, a double-slope S–N curve is constructed.

6. Determining Ice Load Stress Spectrum

The horizontal axis of the curve represents the number of cycles in which ice load impacts on the shaft system, and the vertical axis represents the amplitude of torsional stress generated by the shaft system under ice load. The ice load stress spectrum is closely related to the S–N curve of the shaft system itself in the fields of fatigue analysis. Comparing the ice load stress spectrum with the S–N curve of the shaft system itself under the same number of cycles can predict the fatigue life of the shaft system under specific ice load conditions.

Firstly, based on the rules, it calculates the total number of ice impacts on the propeller ZN_{ice}, where Z is the number of propeller blades. The number of load cycles N_{ice} for each blade is calculated according to Formula (27) [27]:

$$N_{ice} = k_1 k_2 k_3 N_{class} n_n \tag{27}$$

where N_{class} is the reference number of impacts per propeller rotational speed for ice classes, which is 2.1×10^6, k_1 is the propeller location factor, where $k_1 = 1$ for a propeller located on the centerline, k_2 is the submersion factor, which is calculated according to Formula (28), k_3 is the propulsion machinery type factor, where $k_3 = 1$ for fixed thrusters, and n_n is propeller speed during free operation without ice at rated power.

$$k_2 = \begin{cases} 0.8 - f, & f < 0 \\ 0.8 - 0.4f, & 0 \leq f \leq 1 \\ 0.6 - 0.2f, & 1 < f \leq 2.5 \\ 0.1, & f > 2.5 \end{cases} \tag{28}$$

where $f = \frac{h_0 - H_{ice}}{D/2} - 1$, h_0 is the depth of the propeller centerline measured from LIWL, and D is the diameter of the propeller.

According to cumulative damage theory, the stress amplitude corresponding to the number of ice impacts on the propeller during the entire cycle is calculated by Formula (29):

$$\tau_{vice} = \tau_{vmax}\left(1 - \frac{\lg N}{\lg(ZN_{ice})}\right) \tag{29}$$

where τ_{vmax} is maximum torsional stress.

Drawing the ice load stress spectrum according to Formula (29).

7. Fatigue Damage Calculation

The cumulative damage ratio C_{MRD} caused by ice load at resonance speed can be calculated by directly integrating from every part of the S–N curve in Palmgren–Miner linear cumulative damage theory according to Formula (30):

$$C_{MRD} = ZN_{ice}\int_0^{\tau_{vHC}} \frac{f(\tau_{vice}, \tau_{vmax})}{N_2(\tau_{vice})} d\tau_{vice} + ZN_{ice}\int_{\tau_{vHC}}^{\tau_{vmax}} \frac{f(\tau_{vice}, \tau_{vmax})}{N_1(\tau_{vice})} d\tau_{vice} \quad (30)$$

where $f(\tau_{vice}, \tau_{max}) = \frac{\ln(ZN_{ice})}{\tau_{vmax}} e^{-\frac{\tau_{vice}\ln(ZN_{ice})}{\tau_{vmax}}}$, which is the probability density function.

8. Example Calculation

Taking the propulsion shaft system of a real inland waterway vessel as an example, the equivalent parameters for a propulsion shaft are shown in Table 2.

Table 2. The equivalent parameters for propulsion shaft.

Unit Number	Unit Name	Rotational Inertia (kg·m^2)	Torsional Rigidity (N·m/rad)
1	Damper	0.0775	516,100
2	Transmission gear system	0.0003	40,329,996
3	Cylinder.1	0.1160	2,703,000
4	Cylinder.2	0.1282	2,703,000
5	Cylinder.3	0.1282	2,703,000
6	Cylinder.4	0.1282	2,703,000
7	Cylinder.5	0.1282	2,703,000
8	Cylinder.6	0.1272	40,329,996
9	Crankshaft output flange	0.0034	27,189,998
10	Fly.	1.6030	51,200
11	Flexible coupling	0.3510	452,000
12	Gear1	0.2010	11,799,750,000
13	Gear2	0.3400	11,799,750
14	Gear3	0.0400	11,799,750,000
15	Gear4	0.1540	11,799,750
16	Gear5	0.0400	11,799,750,000
17	Gear6	0.1473	528,900
18	Intermediate shaft	0.0188	70,600
19	Tail coupling	0.0603	13,800
20	Prop.	0.5100	

Diesel engine parameters are shown in Table 3.

Table 3. Diesel engine parameters.

No. of Strokes	No. of Cylinders	Cylinder Diameter (mm)	Crank Radius (mm)	Link Length (mm)	Rated Power (kW)	Rated Speed (r/min)	Mechanical Efficiency	Firing Angle (°)
4	6	126	78	253	220	1800	0.89	0-480-240-600-120-360

Propeller parameters are shown in Table 4.

Table 4. Propeller parameters.

Diameter (m)	Pitch (m)	Outer Diameter of Propeller Hub (m)	Design Speed of Propeller (r/min)	Expanded Blade Area Ratio	Pitch Ratio	Trim Angle (°)	Number of Blades
1.0	0.965	0.18	714.29	0.7	0.965	10	4

No.18 intermediate shaft in the system is taken as the research object, its tensile strength σ_b = 480 MPa and yield strength σ_y = 240 MPa. The dimensions of No.18 intermediate shaft are shown in Figure 4.

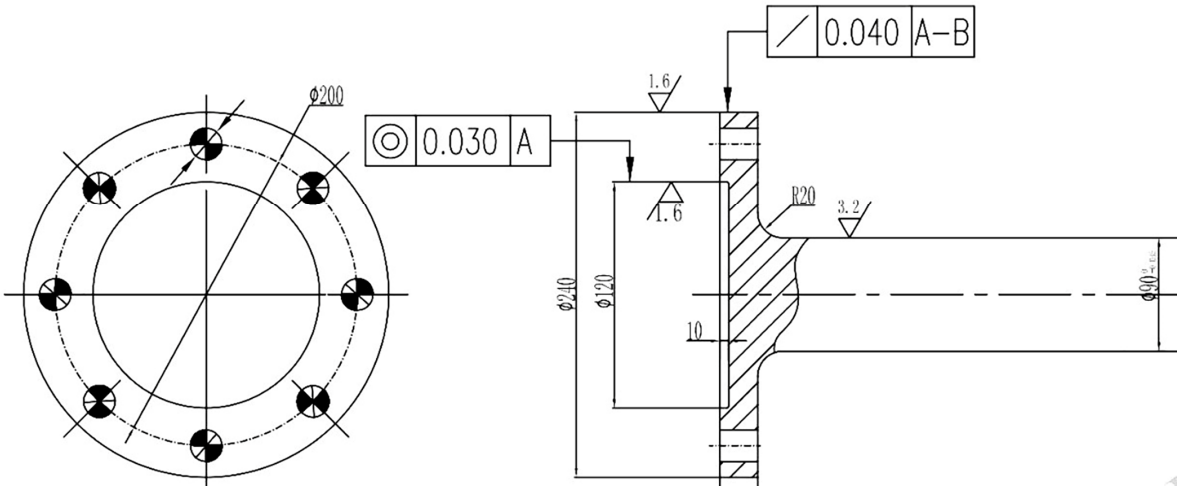

Figure 4. Dimensions of No.18 intermediate shaft.

Firstly, using the field matrix method to calculate the natural frequency of the system's free torsional vibration. The first five natural frequencies calculated by the field matrix method and the Holtz table method are shown in Table 5. After comparison, it is found that the first five natural frequences calculated by the two methods are almost identical.

Table 5. Comparison of calculation results between field matrix and Holtz table.

Order	Field Matrix Method (Hz)	Holtz Table Method (Hz)
1	23.24	23.23
2	40.72	40.69
3	179.26	179.52
4	210.59	210.48
5	424.81	424.59

The low cycle stress and high cycle stress are only related to the characteristics of the shaft system itself. According to the dimension and material properties of No.18 intermediate shaft, the maximum stress of the low cycle and high cycle is calculated as shown in Table 6.

Table 6. Maximum stress of low cycle and high cycle.

	Calculated Value (MPa)	Allowable Value (MPa)
Maximum stress in low cycle	10.60	89.21
Maximum stress in high cycle	1.63	63.37

The first-order natural frequency resonance speed n_c = 1393.8 r/min is taken as research object. Firstly, the maximum torsional stress of the shaft system under cases 1, 2, and 4 are calculated when the maximum design ice thickness H_{ice} = 0.5 m [30]. After programing calculations, the displacement of No.18 intermediate shaft under various cases during the 360° rotation of the propeller and contact with ice is shown in Figure 5.

The velocity of No.18 intermediate shaft under various cases during the 360° rotation of the propeller and contact with ice is shown in Figure 6.

The acceleration of No.18 intermediate shaft under various cases during the 360° rotation of the propeller and contact with ice is shown in Figure 7.

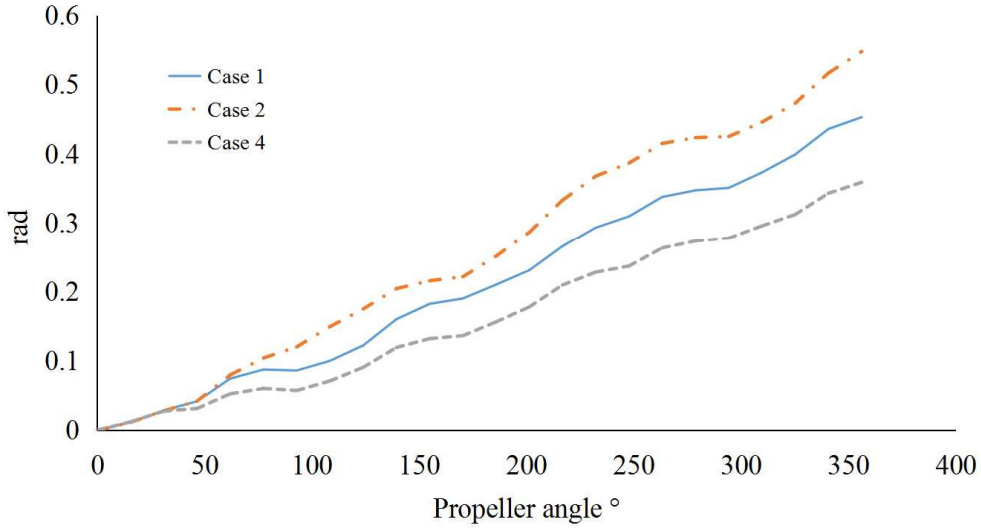

Figure 5. Displacement of No.18 intermediate shaft under three cases.

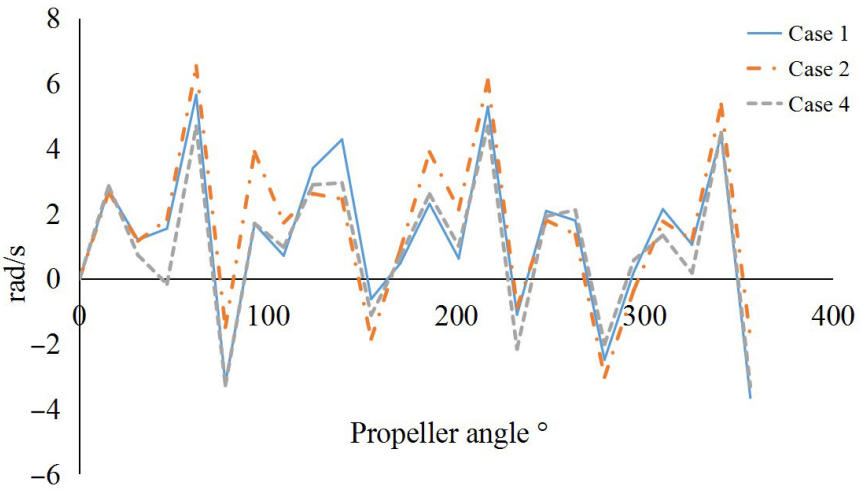

Figure 6. Velocity of No.18 intermediate shaft under three cases.

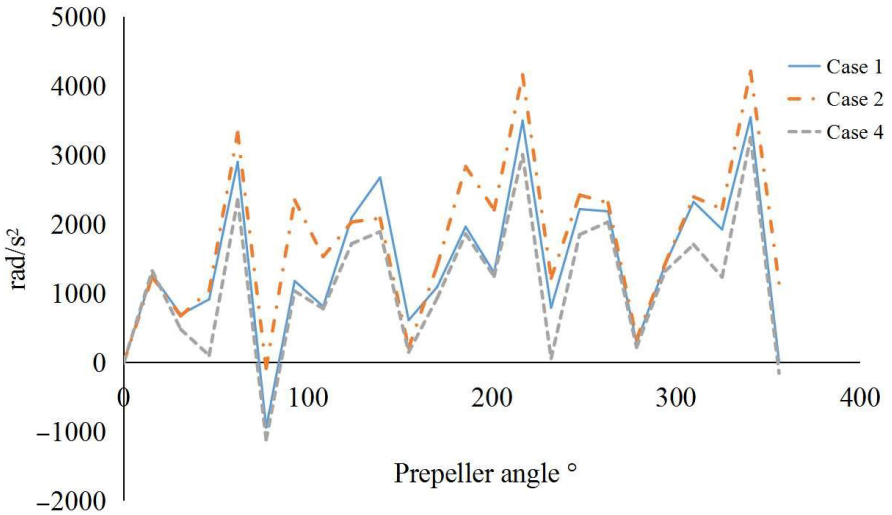

Figure 7. Acceleration of No.18 intermediate shaft under three cases.

Based on the displacement of adjacent mass points on the No.18 intermediate shaft and the dimensions of the shaft, the torsional stress during contact between the propeller rotating 360° and the ice block is calculated, as shown in Figure 8.

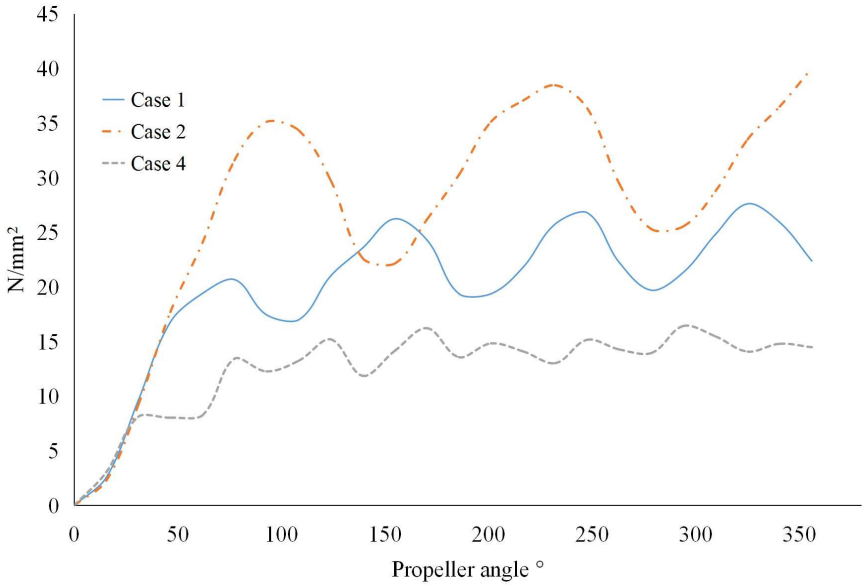

Figure 8. Torsional stress of No.18 intermediate shaft under three cases.

The maximum torsional stress values of the shaft system under three cases are shown in Table 7.

Table 7. Maximum torsional stress of shaft system under three cases.

Case 1 (MPa)	Case 2 (MPa)	Case 4 (MPa)
27.61	40.04	16.64

Due to the fact that the S–N curve is a characteristic of the shaft system itself, the S–N curves for the three cases are the same. It is shown in Figure 9.

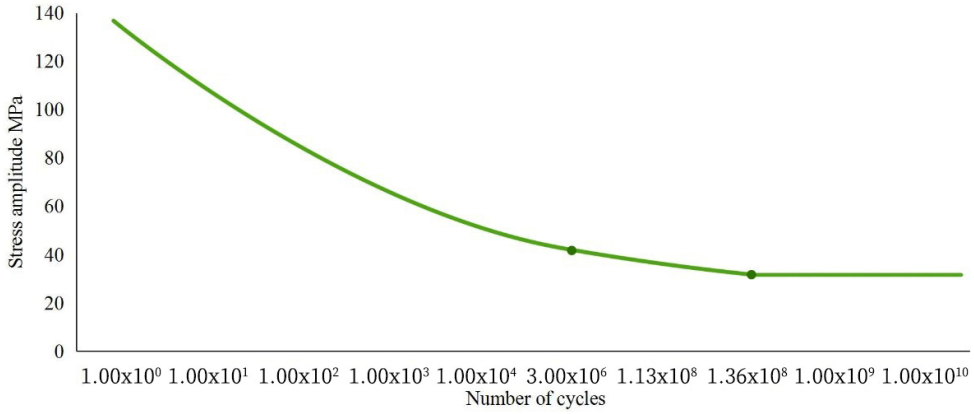

Figure 9. S–N curve of No.18 intermediate shaft.

The drawing of ice load stress spectrum based on the maximum torsional stress of the shaft system under three cases is shown in Figure 10.

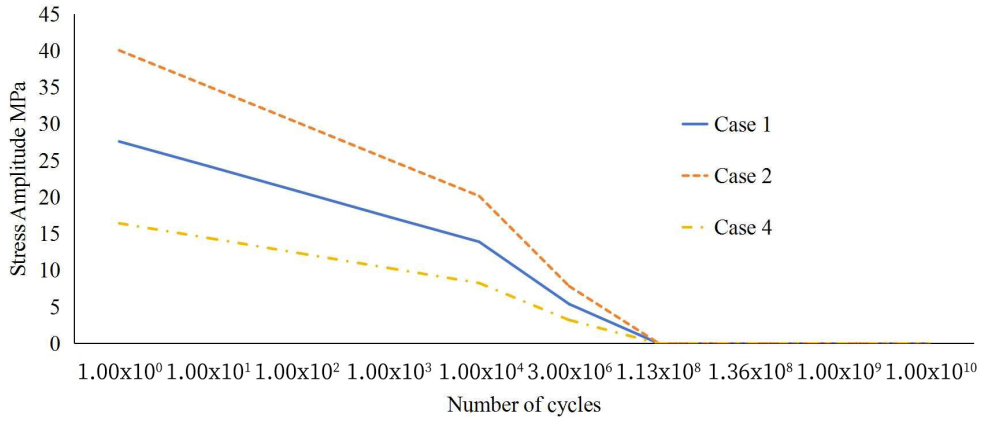

Figure 10. Ice load stress spectrum under three cases.

Finally, based on the linear cumulative damage theory, the cumulative damage ratio of three cases is calculated as shown in Table 8.

Table 8. Cumulative damage ratio under three cases.

Case 1 (MPa)	Case 2 (MPa)	Case 4 (MPa)
7.33×10^{-16}	3×10^{-11}	4.93×10^{-23}

When the maximum design ice thickness is H_{ice} = 0.5 m, by comparing the three cases, it is found that:

(1) The maximum torsional stress of shaft system after ice contact with the propeller far exceeds the low cycle stress and high cycle stress but does not exceed the allowable value;
(2) The maximum torsional stress and cumulative damage ratio of the shaft system increase with the increase in contact time between the ice block and propeller;
(3) The stress amplitude in the ice load stress spectrum under the same number of cycles is much smaller than that in the S–N curve of the shaft system itself, and the cumulative damage ratio is much smaller than 1.

Taking case 1 as the research object, it calculates the maximum torsional stress of the shaft system when the maximum design ice thickness H_{ice} is 0.5 m, 0.8 m, and 1.0 m, respectively. After programing calculations, the displacement of No.18 intermediate shaft under different maximum design ice thicknesses is shown in Figure 11.

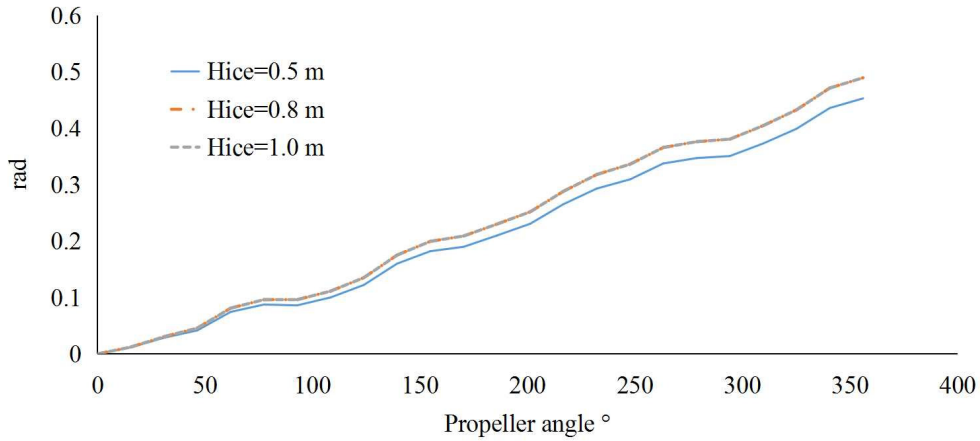

Figure 11. Displacement of No.18 intermediate shaft under three maximum design ice thicknesses.

The velocity of No.18 intermediate shaft under different maximum design ice thicknesses is shown in Figure 12.

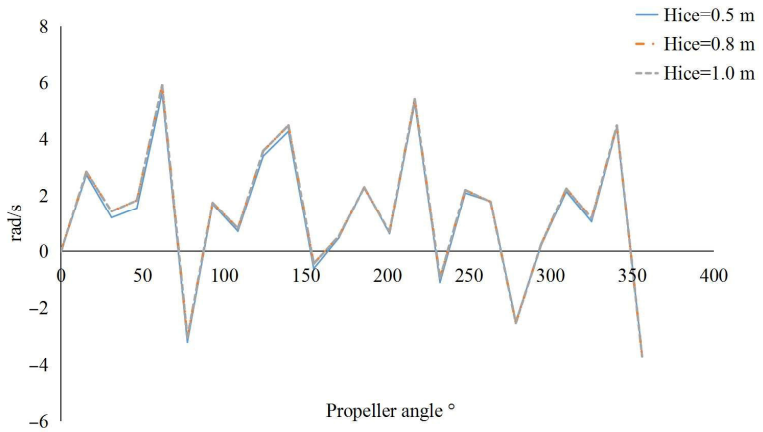

Figure 12. Velocity of No.18 intermediate shaft under three maximum design ice thicknesses.

The acceleration of No.18 intermediate shaft under different maximum design ice thicknesses is shown in Figure 13.

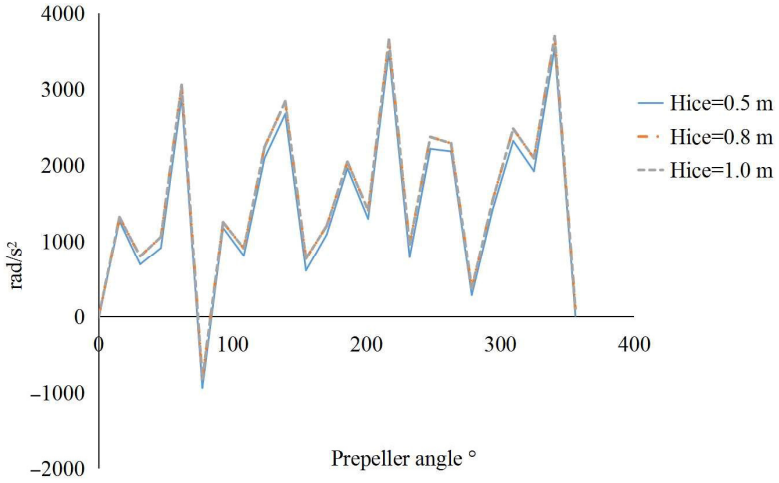

Figure 13. Acceleration of No.18 intermediate shaft under three maximum design ice thicknesses.

The torsional stress is shown in Figure 14.

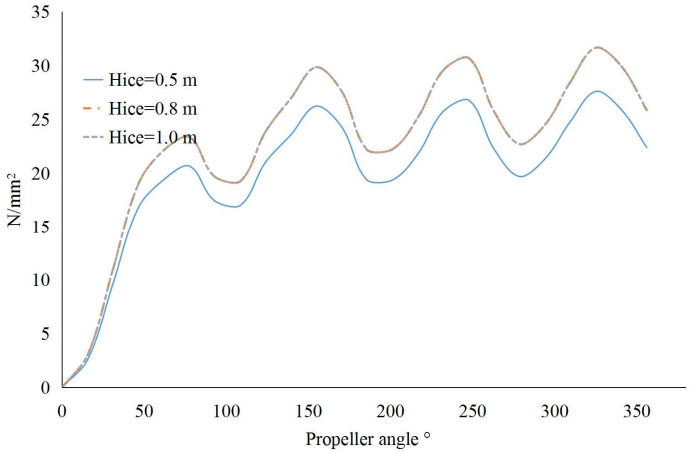

Figure 14. Torsional stress of No.18 intermediate shaft under three maximum design ice thicknesses.

The maximum torsional stress of the shaft system under three maximum design ice thicknesses is shown in Table 9.

Table 9. Maximum torsional stress of shaft system under three maximum design ice thicknesses.

H_{ice} = 0.5 m (MPa)	H_{ice} = 0.8 m (MPa)	H_{ice} = 1.0 m (MPa)
27.61	31.67	31.67

The drawing of ice load stress spectrum based on the maximum torsional stress of shaft system under three maximum design ice thicknesses is shown in Figure 15.

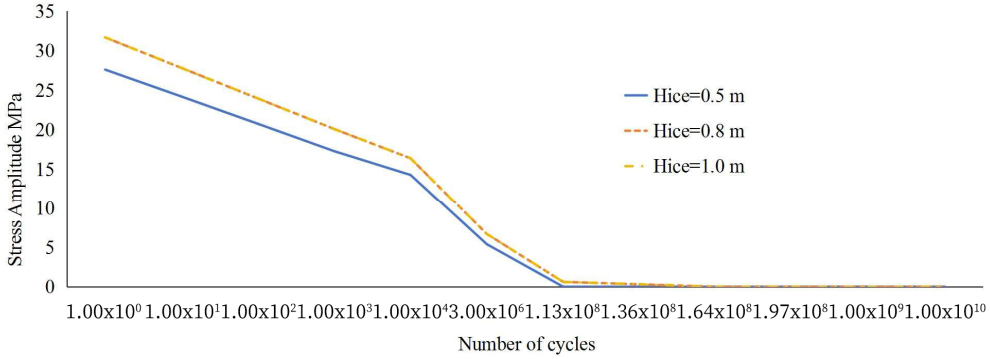

Figure 15. Ice load stress spectrum under three maximum design ice thicknesses.

According to the linear cumulative damage theory, the cumulative damage ratio of three maximum design ice thicknesses is calculated as shown in Table 10.

Table 10. Cumulative damage ratio under three maximum design ice thicknesses.

H_{ice} = 0.5 m	H_{ice} = 0.8 m	H_{ice} = 1.0 m
7.33×10^{-16}	3.78×10^{-14}	3.4×10^{-14}

Under case 1, by comparing the calculation of three maximum design ice thicknesses, it is found that:

(1) The maximum torsional stress and cumulative damage ratio of the shaft system increase with the increase in the maximum design ice thickness.
(2) When H_{ice} = 0.8 m and H_{ice} = 1.0 m, the maximum torsional stress curves of the shaft system under the two maximum design ice thicknesses completely overlap. According to Formula (10), when the maximum design ice thickness exceeds a certain value, the maximum torque of the designed ice block is only related to the properties of propeller itself and is independent of the maximum design ice thickness.
(3) When H_{ice} = 0.8 m and H_{ice} = 1.0 m, the linear cumulative damage ratio is almost the same. According to Formula (28), when the maximum design ice thickness exceeds a certain value, only the submersion factor k_2 changes, while the other coefficients remain completely consistent.
(4) The stress amplitude in the ice load stress spectrum under the same number of cycles is much smaller than that in the S–N curve of the shaft system itself, and the cumulative damage ratio is much smaller than 1.

9. Discussion

This study on the fatigue characteristics of instantaneous torsional stress in the shaft system of inland waterway ships after ice collision with propellers has profound implications for future scientific investigations. It not only reveals the performance changes of

ships in extreme environments but also provides new perspectives and approaches for future research directions.

The impact on future scientific investigations:

Improving ship safety: By conducting in-depth research on the instantaneous torsional stress fatigue characteristics of the shaft system after ice collision with propellers, the safety of ships navigating in ice areas can be more accurately evaluated. This helps prevent ship accidents caused by shaft fatigue and ensures the safety of crew and cargo.

Optimizing ship design: Studying the impact of ice impact on the shaft system can help engineers optimize ship design, especially in terms of propellers and shaft systems. By improving materials and structures, the damage to the shaft system caused by ice impact can be reduced and the durability and reliability of the ship can be improved.

The impact on future research directions:

Expanding research on shaft fatigue: Shaft fatigue is one of the important issues for the safety of ship structures. Through this study, the research field of shaft fatigue can be further expanded, such as the fatigue characteristics of shaft materials and the optimization design of shaft structures.

Promoting interdisciplinary collaboration: This research involves multiple disciplines such as mechanics, materials science, and ship engineering. It will promote cross disciplinary integration between these disciplines and drive the development of interdisciplinary research.

This study on the fatigue characteristics of instantaneous torsional stress in the shaft system of inland waterway ships after ice collision with propellers has opened up a new avenue for scientific investigation. It not only provides new research perspectives and methods but also promotes the development of related technologies and advances in interdisciplinary research. This will help to gain a deeper understanding of the performance changes of ships in extreme environments, providing strong support for future ship design and safety assessments.

There are currently a large number of other scholars studying the maximum torsional stress of the shaft system itself, as well as the instantaneous maximum torsional stress caused by ice loads, but there is little research on the fatigue characteristics under this torsional stress. This article makes up for the research in this field.

10. Conclusions

This research takes the propulsion shaft system of a real inland waterway vessel as an example to study the natural frequency of free torsional vibration of the system. The maximum torsional stress of the intermediate shaft under ice load at resonance speed is calculated using Newmark integration and programing. Based on the maximum torsional stress and fatigue strength analysis theory, the fatigue strength of the intermediate shaft is evaluated, and the following conclusions are obtained:

(1) The low cycle stress and high cycle stress of the shaft system itself are much lower than the allowable stress.
(2) The maximum torsional stress of the shaft system after ice contact with the propeller far exceeds the low cycle stress and high cycle stress, but does not exceed the allowable value.
(3) The maximum torsional stress and cumulative damage of the shaft system increase with the increase in contact time between the ice block and the propeller.
(4) The maximum torsional stress and cumulative damage of the shaft system increase with the increase in the maximum design ice thickness. When the maximum design ice thickness reaches a certain value H_{ice} = 0.8 m, the maximum torsional stress and cumulative damage of the shaft system remain almost unchanged.

(5) The stress amplitude in the ice load stress spectrum under the same number of cycles is much smaller than that in the S–N curve of the shaft system itself, and the cumulative damage ratio is much smaller than 1.

Due to the ice load excitation, the maximum torsional stress of the shaft system increases and the fatigue strength decreases; it is recommended to choose the propeller dimension reasonably based on the maximum design ice thickness of the navigation area to improve the fatigue characteristics of the shaft system. At the same time, ships sailing in ice areas should avoid resonance speed.

Author Contributions: Conceptualization, K.Y. and G.F.; methodology, K.Y.; software, K.Y.; validation, K.Y.; investigation, K.Y.; data curation, K.Y.; writing—original draft preparation, K.Y.; writing—review and editing, K.Y.; visualization, K.Y.; supervision, G.F.; project administration, K.Y.; funding acquisition, G.F. All authors have read and agreed to the published version of the manuscript.

Funding: This research was funded by National Natural Science Foundation of China (Grant No. 52171301).

Institutional Review Board Statement: Not applicable.

Informed Consent Statement: Not applicable.

Data Availability Statement: The data presented in this study are available on request from the corresponding author. The data are not publicly available due to privacy concerns.

Conflicts of Interest: The authors declare no conflicts of interest.

References

1. China Classification Society. *Rules for Construction of Inland Waterway Steel Ships*; People's Communications Publishing House Co., Ltd.: Beijing, China, 2016.
2. Yang, H.; Che, C.; Zhang, J. Transient torsional vibration analysis for ice impact of ship propulsion shaft. *J. Ship Mech.* **2015**, *19*, 177. [CrossRef]
3. Yang, H. Research on Multi-Axial Fatigue Evaluation Method of Polar Ships Under Ice Load. Master's Thesis, Dalian University of Technology, Dalian, China, 2022.
4. Chen, B. The Fatigue Life Analysis of Marine Helical Gear Based on Transient Dynamics. Master's Thesis, Wuhan University of Technology, Wuhan, China, 2017.
5. Wu, L.; Dong, L.; Xu, W. 3D modeling of ship propeller based on MATLAB and ProE. *J. Dalian Marit. Univ.* **2011**, *37*, 17–20.
6. Sun, N.; Yan, C.; Zhang, T. Modeling Method of Propeller Blade Surface Based on Pro/E. *Mech. Eng.* **2010**, *7*, 61–62. [CrossRef]
7. Qian, W.; Wu, C.; Leng, W. Research on automatic geometric modeling and meshing for marine propellers. *Ship Sci. Technol.* **2011**, *33*, 39–43. [CrossRef]
8. Hu, Z. Static Analysis of Propeller Under Ice Loads and Dynamic Response of the Collision Between Ice and Blade. Master's Thesis, Harbin Institute of Technology, Harbin, China, 2014.
9. Wu, X. Analysis of Torsional Vibration of Propulsion Shafting under Ice Load Impact. *SHIP$BOAT* **2020**, *31*, 60. [CrossRef]
10. Xiao, Q.; Chen, B.; Xu, X. Transient vibration calculation of ship propulsion shafting based on ice load dynamic excitation. *J. Ship Mech.* **2020**, *24*, 390.
11. Murawski, L.; Dereszewski, M. Theoretical and practical backgrounds of monitoring system of ship power transmission systems' torsional vibration. *J. Mar. Sci. Technol.* **2020**, *25*, 272–284. [CrossRef]
12. Sibryaev, K.; Gorbachev, M.; Ibadullaev, A. Developing Information Processing Unit Used in Software and Hardware Complex Monitoring Ship Shaft Line Torsional Vibrations. *Vestn. Astrakhan State Tech. Univ.* **2021**, *1*, 22–28. [CrossRef]
13. Kettrakul, P.; Promdirek, P. Failure analysis of propeller shaft used in the propulsion system of a fishing boat. *Mater. Today Proc.* **2018**, *5*, 9624–9629. [CrossRef]
14. Han, H.; Lee, K. Experimental verification for lateral-torsional coupled vibration of the propulsion shaft system in a ship. *Eng. Fail. Anal.* **2019**, *104*, 758–771. [CrossRef]
15. Li, J. The Analysis and Research About Torsional Vibration on Marine Propulsion Shafting of Ship Navigation in Ice. Master's Thesis, Wuhan University of Technology, Wuhan, China, 2016.
16. Gao, J.; Zhang, Y. Ship collision avoidance decision-making research in coastal waters considering uncertainty of target ships. *Brodogradnja* **2024**, *75*, 75203. [CrossRef]

17. Lee, S.; Jung, K.; Ku, N.; Lee, J. A comparison of regression models for the ice loads measured during the ice tank test. *Brodogradnja* **2023**, *74*, 1–15. [CrossRef]
18. Shen, S.; Yao, S.; Guo, H.; Zhang, B.; Yu, T. Study on the standard value of compressive strength of inland river ice flow. *Low Temp. Archit. Technol.* **2015**, *9*, 20–22. [CrossRef]
19. Wang, J.; Zhou, M.; Ding, J.; Sun, H.; Wang, J. Investigation of Fatigue Strength of High Polar-class Propeller. *Shipbuild. China* **2024**, *65*, 1–14.
20. Xu, P.; Wang, C.; Guo, C.; Yang, B.; Su, Y. Experimental study on milling state of unfrozen model ice-propellers. *J. Ship Mech.* **2023**, *27*, 81–96.
21. Chen, P.; Guan, Y.; Yu, Q.; Wang, G.; Ma, G. Numerical simulation and analysis of propeller load of ships sailing in broken ice area. *Ship Sci. Technol.* **2023**, *45*, 15–19. [CrossRef]
22. Wu, Z.; Yi, X.; Xiong, H.; Zhou, Z.; Tian, X. Study on Anti-icing Heat Load Distribution for a Three-Dimensional Propeller. *Trans. Nanjing Univ. Aeronaut. Astronaut.* **2023**, *40*, 688–702. [CrossRef]
23. Liao, P. Research and Software Development About Transient Torsional Vibration on Typical Propulsion Shafting of Ice Ship. Master's Thesis, Wuhan University of Technology, Wuhan, China, 2018.
24. Yang, H. Torsional Vibration Calculation and Analysis for Ice Class Ship. Master's Thesis, Shanghai Jiaotong University, Shanghai, China, 2015.
25. Liao, P.; Zhou, R.; Li, J. Research on Calculation of Transient Torsional Vibration of Diesel Engine Propulsion Shafting in Ice-class Vessel. *Shipbuild. China* **2018**, *59*, 118.
26. Wang, Q. *Torsional Vibration of Engine Crankshaft*; Dalian University of Technology Press: Dalian, China, 1991.
27. China Classification Society. *Rules for Classification of Sea-Going Steel Ships*; People's Communications Publishing House Co., Ltd.: Beijing, China, 2024.
28. DET NORSKE VERITAS. *Calculation of Shafts in Marine Applications*; DET NORSKE VERITAS: Bærum, Norway, 2021.
29. DET NORSKE VERITAS. *Ice Strengthening of Propulsion Machinery and Hull Appendages*; DET NORSKE VERITAS: Bærum, Norway, 2021.
30. Liu, Y. Research on the Bow Type of the Inland-River Icebreaker. Master's Thesis, Harbin Engineering University, Harbin, China, 2010.